

**Kinetic model for surface reconstruction**V. N. Kuzovkov,<sup>1,2,\*</sup> O. Kortlüke,<sup>2</sup> and W. von Niessen<sup>2</sup><sup>1</sup>*Institute of Solid State Physics, University of Latvia, 8 Kengaraga Street, LV 1063 RIGA, Latvia*<sup>2</sup>*Institut für Physikalische und Theoretische Chemie, Technische Universität Braunschweig, Hans-Sommer-Straße 10, 38106 Braunschweig, Germany*

(Received 7 December 2001; published 25 July 2002)

A microscopic kinetic model for the  $\alpha \rightleftharpoons \beta$  [e.g.,  $hex \rightleftharpoons 1 \times 1$  for Pt(100) and  $1 \times 2 \rightleftharpoons 1 \times 1$  for Pt(110)] surface reconstruction is investigated by means of the mean field approximation and Monte Carlo simulations. It considers homogeneous phase nucleation that induces small surface phase defects. These defects can grow or decline via phase border propagation in dependence on the chemical coverage by an adsorbate  $A$  (CO). An asymmetry in the adsorbate surface diffusion from one surface phase to the other gives rise to two critical coverages that determine the intervals of stability of the homogeneous  $\alpha$  phase, the dynamically stable heterogeneous state, and the homogeneous  $\beta$  phase. Both surfaces show a very similar qualitative behavior regarding the phase transitions that are of second order in both cases. As a result the experimentally observed nonlinear island growth rate and the critical coverages can be explained at a quantitative level.

DOI: 10.1103/PhysRevE.66.011603

PACS number(s): 82.65.+r, 64.60.Qb, 81.10.Jt, 82.20.Wt

**I. INTRODUCTION**

The phenomenon of surface reconstruction of Pt single crystal surfaces and the lifting of this reconstruction caused by certain adsorbates such as CO or NO is well known [1–3] and the mechanism has been extensively investigated [2–4]. For reviews see Refs. [5,6]. The Pt(100) surface can undergo a phase transition from the reconstructed (*hex*) phase with a quasi-hexagonal arrangement of the surface atoms to the non-reconstructed ( $1 \times 1$ ) phase. The *hex* phase is more stable when the surface is adsorbate-free while the presence of CO removes the reconstruction and the surface reverts to the  $1 \times 1$  phase. The Pt(110) surface shows a phase transition between the  $1 \times 2$  (reconstructed) and the  $1 \times 1$  (nonreconstructed) surface phases. It turns out that the basic underlying mechanisms are very similar for both surfaces [6]. Therefore it is rather surprising that previous theoretical models treat the reconstruction on the Pt(100) and Pt(110) surfaces quite separately from each other and, moreover, regard the two surfaces as being limiting cases for first- and second-order transitions [5,7,8] in the context of surface reconstruction. On the other hand, in studies on the heterogeneous catalytic CO oxidation on the Pt(100) [9] and Pt(110) [10] surfaces using the so-called mathematical modeling based on the mean field (MF) approximation, the equations that have been used for the description of the two surfaces are formally identical.

In the present paper, we will show that it is possible to describe correctly the reconstruction phenomena on both surfaces with only one model with the same elementary processes and only different parameter values for the individual kinetic transitions such as diffusion coefficients, activation energies, and so on. Therefore, we use the terms  $\alpha$  and  $\beta$  phase for the reconstructed [*hex* on Pt(100),  $1 \times 2$  on Pt(110)] and nonreconstructed surface phase [ $1 \times 1$  in both cases], respectively. Furthermore, our model predicts the

known experimental results such as local, global and critical coverages as well as growth, and nucleation rates as a *result* of the model. This is a decisive improvement compared to previous models, which had to use these as parameters taken from experiment without any further justification.

The paper is organized as follows. In Sec. II, we will shortly discuss the most important results from experiment and previous theoretical models regarding the surface reconstruction of Pt(100) and Pt(110) in the presence of adsorbed CO. In Sec. III, our model is described in detail. In Secs. IV and V the results of the MF approximation and Monte Carlo (MC) simulations, respectively, are presented and discussed. Conclusions are drawn in Sec. VI.

**II. EXPERIMENTAL RESULTS AND PREVIOUS MODELS FOR SURFACE RECONSTRUCTION: A BRIEF REVIEW****A. Critical coverages**

On both the Pt(100) and the Pt(110) surface the dynamically stable coexistence of the reconstructed and nonreconstructed phases can be observed [5,6]. The adsorbate coverage determines the stability of the individual surface phases. For the Pt(110) surface the  $\alpha$  phase is stable for CO coverages below the critical coverage of  $\Theta_{CO} < \Theta_{CO,crit}^{(1)} \approx 0.2$  [11]. For  $\Theta_{CO} > \Theta_{CO,crit}^{(2)} \approx 0.5$  the  $\beta$  phase is stable. The reconstruction of the Pt(110) surface can therefore be described with *two* critical values of the CO coverage. For a theory of the surface reconstruction the first critical point  $\Theta_{CO,crit}^{(1)}$  is more important, because in the case of a high adsorbate coverage additional phenomena such as adsorbate-adsorbate interactions or the coverage dependence of the individual processes determine the behavior of the open system: e.g., the saturation coverage of CO on the  $\beta$  phase is less than one due to repulsive CO-CO interactions [2,3]. A very similar behavior has been observed for the Pt(100) surface. Again, two critical values determine the stability of the  $\alpha$  and  $\beta$  phase. The second critical value is almost equal to the second one for Pt(110), i.e., for  $\Theta_{CO} > \Theta_{CO,crit}^{(2)} \approx 0.5$  the  $\beta$  phase is

\*Electronic address: kuzovkov@latnet.lv

stable [2,3]. The first critical value  $\Theta_{\text{CO,crit}}^{(1)} \approx 0.05$  is much smaller [3]. This critical value seems to depend slightly on the temperature but always remains small. The onset of the nucleation has been observed even for  $\Theta_{\text{CO,crit}}^{(1)} \approx 0.01$  at 387 K [12]. For 500 K the critical coverage has been determined to  $\Theta_{\text{CO,crit}}^{(1)} \approx 0.05$  [3] or  $\Theta_{\text{CO,crit}}^{(1)} \approx 0.08 \pm 0.05$  [13].

In the literature an additional critical coverage  $\Theta_{\text{CO,crit}} \approx 0.3$  for Pt(100) is often used in combination with the above-mentioned ones [3,6]. But this critical point has a completely different physical meaning and determines the value of the total CO coverage for which the different surface phases are energetically equivalent, i.e., the coverage of the two phases on the surface is almost equal. This should not be confounded with the real critical values mentioned above.

### B. The heterogeneous state

In the interval  $\Theta_{\text{CO,crit}}^{(1)} < \Theta_{\text{CO}} < \Theta_{\text{CO,crit}}^{(2)}$ , a heterogeneous state exists on both surfaces. In this heterogeneous state islands of both the  $\alpha$  and the  $\beta$  phase coexist on the surface, i.e., this heterogeneous state is *dynamically stable*. In experiment, segregation of the individual phases has not been observed and the surface structure remains statistically unchanged with a certain mean size of the phase islands. In our opinion this fact—which has been ignored in most theoretical studies to date—is of paramount importance and should be a fundamental aspect of future theories.

The mean size and the shape of the islands depends on the global CO coverage  $\Theta_{\text{CO}}$ . But the global coverage has no influence on the local properties of the phases. For example, during the CO-induced  $\alpha \rightarrow \beta$  phase transformation on Pt(100), the local CO coverage on the  $\beta$  phase is high, approximately  $\Theta_{\text{CO}}^{(\beta)} \approx 0.5$ , while on the remaining areas of the  $\alpha$  phase the local CO coverage is low, typically less than  $\Theta_{\text{CO}}^{(\alpha)} \approx 0.03$  [14,15]. These local coverages are almost independent of the total CO coverage  $\Theta_A$  [14,15] and seem to coincide with the values of the critical CO coverages, i.e.,  $\Theta_{\text{CO}}^{(\alpha)} \approx \Theta_{\text{CO,crit}}^{(1)}$  and  $\Theta_{\text{CO}}^{(\beta)} \approx \Theta_{\text{CO,crit}}^{(2)}$ .

The large ratio of the local coverages of  $\Theta_{\text{CO}}^{(\beta)}/\Theta_{\text{CO}}^{(\alpha)} \approx 10\text{--}20$  can be taken as an attribute of the Pt(100) surface. If we assume that the same properties hold for the Pt(110) surface we obtain a much smaller ratio of  $\Theta_{\text{CO}}^{(\beta)}/\Theta_{\text{CO}}^{(\alpha)} \approx 2.5$ . The inhomogeneous distribution of the CO molecules can be explained with the difference in the adsorption energies for CO adsorption on the  $\alpha$  and  $\beta$  phase [2,3,6]. This then leads to asymmetric diffusion where the rate of the CO jumps from the  $\beta$  phase to the  $\alpha$  phase is much smaller compared to the rate of the reverse jumps. The phase border can therefore be regarded as a sort of membrane that operates only in the *physical direction*, i.e., it supports diffusion from the  $\alpha$  phase to the  $\beta$  phase but hinders the reverse process.

### C. Critical surface activity below $\Theta_{\text{CO,crit}}^{(1)}$

It has been shown by Hopkinson *et al.* [14,15] in a study on the island growth dynamics in adsorbate-induced surface reconstruction that the growth rate of the  $\beta$  phase strongly

increases with the local CO coverages on the  $\alpha$  phase  $\Theta_{\text{CO}}^{(\alpha)}$  even for values below or at the critical point and that the surface shows a *critical activity* for reconstruction for  $\Theta_{\text{CO}} \rightarrow \Theta_{\text{CO,crit}}^{(1)}$ , although the  $\alpha$  phase is stable for  $\Theta_{\text{CO}}^{(\alpha)} < \Theta_{\text{CO,crit}}^{(1)}$ . It was stated that the growth rate  $r_g$  apparently obeys a power law  $r_g \propto [\Theta_{\text{CO}}^{(\alpha)}]^\nu$  with an exponent of  $\nu = 4.5 \pm 0.4$  with respect to the CO coverage on the  $\alpha$  phase [15]. This actually means that the  $\beta$  phase has to be present for  $\Theta_{\text{CO}} < \Theta_{\text{CO,crit}}^{(1)}$ , but only as microscopic nuclei that are induced on an atomic length scale and therefore are unimportant on the macroscopic length scale, which has been observed in the experiments in Refs. [14,15]. Independent of the interpretation of the experimental results the above-mentioned critical activity is an attribute of the surface reconstruction that is typical only for certain critical phenomena. Particularly, it cannot be described within the theory of first-order phase transitions.

### D. The problem of the nucleation

It is an experimental fact that the surface reconstruction passes through a nucleation process as soon as a certain CO coverage is reached, i.e., the phase is not changed at once on the whole surface but rather builds small nuclei that grow until the new phase is established. Because of the experimental results about the stability of the individual surface phases mentioned above it has been assumed, though not conclusively shown, that the nucleation has to be heterogeneous [14,15], i.e., one assumes that the  $\beta$  phase nuclei are only formed if the local CO coverage in a certain surface domain exceeds a threshold. In Refs. [14,15] four or five CO molecules are assumed to be involved in a concerted nucleation step. The  $\alpha$  phase nucleation is then assumed to occur in small surface domains where the local CO coverage drops below a second threshold. But there are some uncertainties about the validity of this assumption. On Pt(110) the value of the critical coverage is large ( $\Theta_{\text{CO,crit}}^{(1)} \approx 0.2$ ) and fluctuations in the local CO coverage may render possible such a concerted step. Nevertheless a kinetical or statistical model is very much in demand to explain these critical coverages. On the other hand, on Pt(100) the value of the critical coverage for the nucleation of the  $\beta$  phase is so small ( $\Theta_{\text{CO,crit}}^{(1)} \approx 0.05$ ) and CO surface diffusion is so fast that it is almost impossible to find an aggregation of four or five CO molecules near one surface site. Therefore it is not clear how local fluctuations in an already low CO coverage shall show such a high activity. In addition, in scanning tunnel microscope studies by Ritter *et al.* [16] and Gritsch *et al.* [4] the nucleation seems to be homogeneous, because the growing  $\beta$  islands were distributed randomly over a terrace without preferential growth from a monoatomic step that was imaged on the initial  $\alpha$  surface.

### E. First-order phase transition models

Because of the very small value of  $\Theta_{\text{CO,crit}}^{(1)}$  on Pt(100) it has been assumed that the surface phase transition on Pt(100) has to be a first-order phase transition. In the theory of first-order phase transitions the coexistence of individual phases

is a general phenomenon. Independent of a specific model definition one can expect to obtain different coverages on different phases, and by using free parameters it is possible to quantitatively fit the critical coverages to experimental results. This has been studied very recently [7]. But models for a first-order phase transition in surface reconstruction encounter some difficulties.

(i) All models considering a phase transition of first order lead to a segregation of the individual phases, independently of their specific definition. Therefore a heterogeneous state is *not* dynamically stable but (asymptotically) transforms into two completely separated phases. This generally occurs via growth of large phase islands at the expense of smaller ones and has been confirmed in a study by Zhdanov [17]. In this study the mean size  $R$  of the larger islands follows the well-known Lifshitz-Slyozov law  $R \propto t^{1/3}$ , i.e., the heterogeneous structures shown in Refs. [8,17] will not exist for longer simulation times.

(ii) Systems showing first-order phase transitions do not show any critical activities near the critical points. Therefore an explanation of the experimental results about the critical surface activity in Refs. [14,15] is impossible.

#### F. Methodical remarks

Statistical models are very popular because it is hoped that with the definition of the lattice variables and the corresponding Hamiltonian of the system it is possible to completely describe the surface reconstruction with all the individual processes such as nucleation, island growth, and so on. The decisive disadvantage of models with first order phase transitions is that purely statistical results obtained with the MF or other simple approximations are results for the steady state, i.e., results for a system with complete segregation. In this context information about phase distributions is of no use. The change from a complete statistical model to a model considering kinetic transitions for adsorption, desorption, and diffusion, and the change of local variables in general is an important improvement that renders possible the study of the evolution of the system.

A further disadvantage of statistical models is that certain terms get mixed: the term of a stable site in a certain state and the term of the corresponding phase, e.g., the  $\alpha$  state and the term of an  $\alpha$  phase. In the lattice model in Ref. [7] a lattice site can exist in a “stable” ( $\alpha$ ) or a “metastable” ( $\beta$ ) state in connection with the CO coverage on this site. But in the statistical theory the term “phase” corresponds to a specific solution of the statistical equations with a certain *distribution* of the  $\alpha$  and  $\beta$  sites and an additional CO coverage. Therefore the terms of CO on a stable  $\alpha$  site and CO on the  $\alpha$  phase are not identical. This may introduce some misunderstanding into the interpretation of the simulation results because the borders of the phases are undefined from the statistical point of view and cannot be observed. One only sees the borders between “stable” and “metastable” domains. Methodically, it would be better to define a model where the terms of the  $\alpha$  ( $\beta$ ) phase and of sites in the  $\alpha$  ( $\beta$ ) state are identical and can be used independently of the CO coverage.

In our opinion the consideration of energetic interactions is important for models to describe experimental results at a quantitative level. But in the context of lattice gas models for surface reactions the introduction of adsorbate-adsorbate and adsorbate-surface interactions seems to be premature today. First one should find the simplest possible model that correctly describes the essential physical properties of the systems, which have been experimentally investigated. Such a model should be available in the near future because the number of studies on surface reactions based on lattice gas models is strongly increasing [7,18–24]. Then, in a second step one can gradually increase the number of elementary processes and/or free parameters of the model. Today, the consideration of energetic interactions has mainly two consequences.

(i) The computing power that is needed for the simulation increases drastically. This limits the models to small lattices and rather short simulation times.

(ii) The second consequence is much more important. The energetic interactions on the surface are practically unknown because experiments mix a lot of processes and can only give macroscopic results. On the other hand, theoretical models based on *ab initio* methods are limited to rather small systems that cannot cover the complex microscopic picture yet. Therefore today the introduction of energetic interactions into lattice models leads to a large number of free parameters, which render possible the fitting to experimental results but may hide the real physics and therefore may lead to a partly wrong picture.

### III. THE MODEL

#### A. General aspects

The basic model has been introduced and described in detail elsewhere [18–20], where it has been studied as a standard model for the oscillating CO oxidation on the Pt(100) and the Pt(110) surfaces. In this model the CO diffusion process has been regarded independent of the surface phase. Here we consider the closed CO/Pt(100) and CO/Pt(110) systems, i.e., we consider Pt single crystal surfaces with a constant CO coverage and ignore CO adsorption and CO desorption. This is feasible because the consideration of CO adsorption and desorption on the  $\alpha$  and  $\beta$  phase would lead to only very small fluctuations and quantitative changes in the CO coverage but would introduce four additional free parameters. The modeling of the CO diffusion process depends on the surface phase as will be shown below. In addition the model considers homogeneous surface phase nucleation and island growth via phase border propagation. Our model is defined kinetically instead of statistically. This Markovian-type model is completely defined via its state variables and the transitions that can occur. These transitions are connected with corresponding kinetic rates that define the time scale. The kinetic MC computer simulations are based on the pair algorithm that is explained in details in Ref. [25].

#### B. Lattice states

The homogeneous  $\alpha$  and  $\beta$  surface phases correspond to the regular arrangements of the substrate atoms of the recon-

structed and nonreconstructed surface, respectively. The phases correspond to local minima of the configuration energy and therefore should be stable against certain fluctuations (e.g., thermal oscillations). The stability of the phases depends on the adsorbate coverage. Therefore we consider both phases as metastable. Regarding the lattice states our kinetic model in principal is very similar to statistical models [7]. Each lattice site exists in the  $\alpha$  or  $\beta$  state, respectively. In addition the sites can be covered with  $A$  (i.e., CO) or can be vacant (0). Therefore the state of a lattice site can be given by  $X^\chi$  with  $X=0, A$  and  $\chi=\alpha, \beta$ .

In our MC simulations, we exclusively use the regular square lattice with the coordination number  $z=4$  to model the surface of the catalyst, although the reconstructed phases on the real catalysts (*hex* and  $1\times 2$ ) have a different geometry (triangular and the so-called “missing row” geometry). In our model only the different physical but not geometrical properties of the phases are considered because it is impossible to give a *local* geometric specification of the phase. The geometry plays only a minor role and leads only to small quantitative changes. This is known (a) from experimental investigations, [e.g., the completely different behavior of the NO dissociation on Pt(111) and Rh(111), although both surface have almost identical geometries], (b) from an investigation of the Ziff, Gulari, Barshad (ZGB) model [26] by Meakin and Scalapino [27], and (c) from our own studies of the present and related models that we implemented on the square and triangular lattice [21]. In our simulations these lattices lead to similar results even at a quantitative level. The results of a model with changes in the local surface geometry should lie in between the results as an interpolation of the two regular lattices.

In addition, we set the lattice constant  $a=1$  in order to be able to compare the individual processes besides leading to simpler expressions.

### C. Kinetic rates

The term metastability simply means that in addition to the thermal oscillations there exists an additional cooperative process that is connected with mass transport. This process is the formation of an  $\alpha$  defect in an otherwise homogeneous  $\beta$  phase (or vice versa). This defect is a primary nucleus and arises from a rare fluctuation but can grow to a new mesoscopic phase under certain conditions, because the further development of these nuclei strongly depends on the local chemical coverage at the moment of nucleation. We model this process as a spontaneous nucleation ( $\alpha\rightarrow\beta$  or  $\beta\rightarrow\alpha$ ) completely independent of the phase and the coverage of the nearest-neighbor (NN) sites and independent of the coverage of the site itself. This is in clear contrast to previous theoretical models where heterogeneous nucleation is dependent on the coverage been used. We will show that our homogeneous nucleation process leads to primary phase defects in an otherwise homogeneous phase. These defects grow or vanish depending on the local coverage. Therefore the homogeneous nucleation in combination with the phase border propagation can appear to be heterogeneous. Because the nucleation is a very rare process we connect this step with a

very small transition rate  $\gamma$ . The homogeneous nucleation is the origin of a dynamically stable heterogeneous state (see below). The advantage of a small nucleation rate is that we can use a heterogeneous state as our initial condition in order to neglect the nucleation process in a first approximation. After the investigation of our model without nucleation we will return to this process and study its influence on the system.

In our present model we assume the phase gradient (phase border) to be the basic reason for the temporal evolution of the heterogeneous state. The phase gradient as an inhomogeneity increases the configurational energy of the system compared to a system with a globally homogeneous phase. Therefore the system will try to reach such a homogeneous surface phase whose type depends on the chemical coverage. In contrast to previous models (see Ref. [19] for a detailed discussion) we assume that the coverage is only important directly at the phase border, i.e., only the very local coverage has an influence on the growth and decline of the phase islands. This growth and decline is modeled as a phase border propagation. Consider two NN sites with the phase states  $\alpha\beta$ . The transition  $\alpha\beta\rightarrow\beta\beta$  ( $\alpha\beta\rightarrow\alpha\alpha$ ) occurs if at least one (none) of the two sites is covered with  $A$ . The corresponding transition rate for both transitions is given by  $V/z$ . Actually, the results for the reconstruction given below are independent of  $z$  and we choose this transition rate in order to eliminate the factor  $z$  in the equations. MC simulations [28] have shown that the maximum of the phase island growth rate is  $v_{\max}=0.59V$  (or  $v_{\max}=0.59aV$  for  $a\neq 1$ ) for a  $\beta$  nucleus in a homogeneous  $\alpha$  phase completely covered with  $A$  or an  $\alpha$  nucleus in a homogeneous  $\beta$  phase with no chemical coverage.

This phase border propagation differs from the previous models where a mean chemical coverage is assumed to have an influence on the phase of an arbitrarily chosen mesoscopic lattice domain. This assumption has the disadvantage that a simple and compact formulation of the elementary processes is not possible. In our model only the  $A$  particles (CO) directly at the phase border influence the phase state of the system. This might appear to be paradoxical at first sight, especially in the context of the critical coverages mentioned above. But we will show that this model is able to explain the observed phenomena, and, even more important is to connect the individual experimental facts such as critical coverages [2,3] and the island growth kinetics [14,15].

It is a known fact that surface diffusion is very fast compared to other surface processes even at ambient temperatures. The surface reconstruction should be independent of the values of the diffusion rate and only the statistics of the presence of CO at the phase borders should be important for the reconstruction. These statistics are not defined by the absolute value of the diffusion rate but by its symmetry regarding the diffusion from one phase to the other. In the simplified model for the oscillating CO+O<sub>2</sub> reaction [19], we defined the diffusion of  $A$  simply by the process  $A^X0^{\chi'}\rightarrow 0^X A^{\chi'}$  with rate  $D$  completely independent of the phase states  $\chi, \chi'=\alpha, \beta$  of the involved surface sites. Note that by using the general units  $\mathcal{D}_A=a^2D/z$  is the diffusion constant for  $A$  diffusion, i.e.,  $D$  corresponds to the frequency factor of

the diffusion. In the present study, we extend the modeling of the diffusion process in agreement with experiment. It is known that the CO diffusion from the  $\beta$  to the  $\alpha$  phase is strongly hindered because of the higher adsorption energy of CO on the  $\beta$  phase [14,15], i.e., the phase border corresponds to a sort of membrane [28,29] that introduces a strong asymmetry into the diffusion process from one phase to the other. This effect does not occur for diffusion on homogeneous phases. Therefore we get four diffusion rates  $D_{\alpha\alpha}, D_{\beta\beta}, D_{\alpha\beta}$ , and  $D_{\beta\alpha}$  for the diffusion  $A^{\chi}0^{\chi'} \rightarrow 0^{\chi}A^{\chi'}$  with  $\chi, \chi' = \alpha, \beta$ . For very fast diffusion ( $D_{\chi\chi'} \rightarrow \infty$ ) the values of  $D_{\alpha\alpha}$  and  $D_{\beta\beta}$  are not so important because only the asymmetry  $D_{\alpha\beta} \neq D_{\beta\alpha}$  determines the distribution of  $A$  on the individual phases and more important also at the phase borders. This then determines the phase border propagation. Furthermore, we will show that this asymmetry also determines the type of the phase transition of the surface reconstruction. In order to keep the number of free parameter as low as possible we set  $D_{\alpha\alpha} = D_{\beta\beta} = D$  in our simulation. For the diffusion at the phase border, we use  $D_{\alpha\beta} = D(1 + \kappa)$  and  $D_{\beta\alpha} = D(1 - \kappa)$  with

$$\kappa = \frac{D_{\alpha\beta} - D_{\beta\alpha}}{D_{\alpha\beta} + D_{\beta\alpha}} \quad (1)$$

as a dimensionless parameter for the diffusion asymmetry. In the *physically relevant* interval  $\kappa \in (0, 1)$  the jump of  $A$  particles from the  $\alpha$  to the  $\beta$  phase is preferred, although the investigation of the interval  $\kappa \in (-1, 0)$  is also possible from the *mathematical* point of view. If we assume that the different diffusion processes have the same frequency factors and only different activation energies, we get

$$\kappa = \tanh\left(\frac{\Delta E}{2k_B T}\right), \quad (2)$$

where  $\Delta E$  and  $k_B$  are the difference in the activation energy and the Boltzmann's constant, respectively. This renders possible the investigation of the influence of the temperature  $T$ .

In our present simulation we use the regular square lattice with side length  $L = 256$  as a model of the catalyst surface and the following parameter values as standard values. Because the time scale can be arbitrarily chosen we set  $V = 1$ . A fast diffusion means  $D \gg V$  with the limit  $D \rightarrow \infty$ , but it has been shown [30] that already for values  $V/D \sim 10^{-2}$  saturation phenomena occur. Therefore we can choose  $D = 100$  as our standard value for the diffusion rate. The weak nucleation as a very rare process means  $\gamma/V \ll 1$ . In order to get statistically robust results we use  $\gamma = 10^{-3}$ . Smaller values lead to almost the same mean values of the results presented below but give rise to much larger fluctuations.

#### IV. MEAN FIELD ANALYSIS

##### A. Chemical and phase coverages

Let  $C_X^\chi$  be the probability to find a lattice site in state  $X^\chi$ . This corresponds to the macroscopic density or concentration. Then the following sum rules hold:

$$\sum_{X,\chi} C_X^\chi = 1,$$

$$\sum_X C_X^\chi = \Theta_\chi,$$

$$\sum_\chi C_X^\chi = \Theta_X,$$

where  $\Theta_\alpha = 1 - \Theta_\beta$  are the phase densities and  $\Theta_A + \Theta_0 = 1$  are the macroscopic surface coverages of sites covered with  $A$  or vacant sites, respectively. We consider a closed system with  $\Theta_A$  constant (see above). The introduction of two variables  $\theta$  and  $\psi$  with  $\theta \equiv \Theta_\beta$  and  $C_A^\beta = \Theta_A \psi$  simplifies the analysis in the framework of the MF approximation. The other probabilities are now given by  $C_A^\alpha = \Theta_A(1 - \psi)$ ,  $C_0^\beta = \theta - \Theta_A \psi$ , and  $C_0^\alpha = (1 - \theta) - \Theta_A(1 - \psi)$ . The equation for the surface phase coverages contains only the nucleation  $\gamma$  and the phase border propagation  $V$  and can now easily be given in the MF approximation:

$$\frac{d\Theta_\beta}{dt} = \gamma(\Theta_\alpha - \Theta_\beta) + V[C_A^\alpha C_A^\beta + C_A^\alpha C_0^\beta + C_0^\alpha C_A^\beta - C_0^\beta C_0^\alpha] \quad (3)$$

or

$$\frac{d\theta}{dt} = \gamma(1 - 2\theta) + V[2\Theta_A(\theta + \psi - 2\theta\psi) - 2\Theta_A^2\psi(1 - \psi) - \theta(1 - \theta)]. \quad (4)$$

Considering an infinitely fast diffusion in the adiabatic approximation we get only an algebraic equation instead of a second differential equation because in the dynamical steady state the number of  $A$  particles diffusing from the  $\alpha$  to the  $\beta$  phase is equal to the number of  $A$  particles that diffuse in the reverse direction:

$$D_{\alpha\beta} C_A^\alpha C_0^\beta = D_{\beta\alpha} C_0^\alpha C_A^\beta. \quad (5)$$

It can clearly be seen that in the context of the MF approximation no information can be obtained for diffusion jumps on one surface phase. Introducing the variables  $\theta$  and  $\psi$  in Eq. (5), we get

$$\theta = \psi \frac{(1 - \kappa) + 2\kappa\Theta_A(1 - \psi)}{(1 + \kappa) - 2\kappa\psi}. \quad (6)$$

The combination of the macroscopic densities for both the phase and the coverage can give information about the mean coverages on the individual surface phases, e.g.,  $\Theta_A^{(\chi)} = C_A^\chi / \Theta_\chi$  is the mean  $A$  density on the  $\chi$  phase. This leads to

$$\Theta_A^{(\beta)} = \Theta_A \frac{\psi}{\theta} \quad \text{and} \quad \Theta_A^{(\alpha)} = \Theta_A \frac{1 - \psi}{1 - \theta}.$$

Without the diffusion asymmetry at the phase border ( $\kappa = 0$ )  $\theta = \psi$  holds and there is no correlation between the

phase and the chemical coverage and we get  $\Theta_A^{(\alpha)} = \Theta_A^{(\beta)} = \Theta_A$ , i.e., the mean local  $A$  coverages on the individual surface phases are given by the global  $A$  coverage. For  $\kappa > 0$  a correlation exists and  $\Theta_A^{(\alpha)} \neq \Theta_A^{(\beta)}$  holds.

### B. Phase border propagation without nucleation

Let us first assume that the nucleation process has created a heterogeneous phase distribution. We can now neglect the nucleation ( $\gamma=0$ ) and investigate the stability of this heterogeneous state. In the simplest case with  $\kappa=0$  and  $\theta=\psi$ ,

$$\frac{d\theta}{dt} = V[1 - 2(1 - \Theta_A)^2]\theta(1 - \theta) \quad (7)$$

follows from Eq. (4). In this case one single critical density of  $A$  exists. For  $\Theta_A < \Theta_{A,\text{crit}}$  with  $\Theta_{A,\text{crit}} = 1 - (1/\sqrt{2}) \approx 0.293$  the  $\alpha$  phase is stable, whereas for  $\Theta_A > \Theta_{A,\text{crit}}$  the  $\beta$  phase is stable.

For  $\kappa \neq 0$  with  $\gamma=0$  in Eqs. (4) and (6) this single critical coverage splits up into two critical coverages

$$\Theta_A^{(1)}(\kappa) = \frac{1 - \kappa}{2 - \kappa + \sqrt{2 - \kappa^2}} \quad (8)$$

and

$$\Theta_A^{(2)}(\kappa) = \frac{1 + \kappa}{2 + \kappa + \sqrt{2 - \kappa^2}}, \quad (9)$$

with the very simple relation  $\Theta_A^{(1)}(\kappa) = \Theta_A^{(2)}(-\kappa)$ . The homogeneous  $\alpha$  phase is stable for  $\Theta_A < \Theta_A^{(1)}(\kappa)$ , where  $\theta = \psi = 0$  holds. The homogeneous  $\beta$  phase is stable for  $\Theta_A > \Theta_A^{(2)}(\kappa)$  with  $\theta = \psi = 1$ . Between these critical points with  $\Theta_A^{(1)}(\kappa) < \Theta_A < \Theta_A^{(2)}(\kappa)$  a heterogeneous state exists with

$$\theta = \Theta_\beta = \frac{\Theta_A^{(2)}(\kappa) - \Theta_A}{\Theta_A^{(2)}(\kappa) - \Theta_A^{(1)}(\kappa)} \quad (10)$$

and with constant  $A$  coverages on the individual phases *independent of the total  $A$  coverage*, i.e., in this heterogeneous state only the phase coverages vary. The  $A$  coverages on the individual phases are given by the critical values

$$\Theta_A^{(\beta)} = \Theta_A^{(2)}(\kappa) \quad \text{and} \quad \Theta_A^{(\alpha)} = \Theta_A^{(1)}(\kappa).$$

Very surprisingly the solution for the heterogeneous state given by Eq. (10) has the same structure as the well-known Maxwell rule in the theory of first-order phase transitions, i.e., our system has the properties of a system showing a first-order phase transition although it actually *does not show a first-order phase transition* (see Table I).

The dependence on  $\kappa$  can be easily investigated. For  $\kappa \rightarrow 1$  we get  $\Theta_A^{(1)}(\kappa) \rightarrow 0$  and  $\Theta_A^{(2)}(\kappa) \rightarrow 0.5$ . This enables us to fit our model to experimental data and to estimate the difference in the activation energy for the diffusion between the  $\alpha$  and the  $\beta$  phase using Eq. (2). Because the experimental critical values for CO/Pt(100) have been obtained with

TABLE I. The assumed value of the critical  $A$  coverage  $\Theta_A^{(1)}(\kappa)$  for 400 K leads to the value of  $\kappa$  and the difference in the activation energy  $\Delta E$  for both directions of the  $A$  diffusion between the  $\alpha$  and  $\beta$  phase. This then can be used to calculate the values for a higher temperature of 500 K via Eq. (2).

| 400 K                    |          | 500 K                    |          | $\Delta E(\text{kJ/mol})$ |
|--------------------------|----------|--------------------------|----------|---------------------------|
| $\Theta_A^{(1)}(\kappa)$ | $\kappa$ | $\Theta_A^{(1)}(\kappa)$ | $\kappa$ |                           |
| 0.010                    | 0.980    | 0.024                    | 0.950    | 15.20                     |
| 0.030                    | 0.936    | 0.055                    | 0.878    | 11.35                     |
| 0.050                    | 0.890    | 0.080                    | 0.813    | 9.44                      |

large errors we simply assume different critical  $A$  coverages at 400 K, which are of the same order as the experimental data [12–15]. These are used in Eq. (8) in order to obtain the value of  $\kappa$  for 400 K, which in turn gives the difference in the activation energy  $\Delta E$  by using Eq. (2). The same equation is then solved for  $T=500$  K and leads to the values of  $\kappa$  and  $\Theta_A^{(1)}(\kappa)$  [Eq. (8)]. As can be seen in Table I our model predicts slightly higher values of the critical coverage for 500 K, which are in good agreement with experiment, whereas the second critical value remains almost constant at  $\Theta_A^{(2)}(\kappa) \approx 0.48$ , which also agrees with  $\Theta_{\text{CO,crit}}^{(2)} \approx 0.5$  obtained from experiment. In addition, the difference in the activation energy can be estimated to be of the order of about 10 kJ/mol. If we assume  $\Theta_A^{(1)}(\kappa) = 0.200$  for CO/Pt(110) the value of  $\kappa$  calculates to  $\kappa = 0.41$  and results in  $\Delta E \approx 3$  kJ/mol, i.e., both the Pt(100) and Pt(110) surface do not show a qualitative but only a quantitative difference that, however, is not very large. The second critical value is  $\Theta_A^{(2)}(\kappa) = 0.375$ . This is somewhat smaller than the measured value of  $\Theta_{\text{CO,crit}}^{(2)} = 0.5$ , but both experimental values for Pt(110),  $\Theta_{\text{CO,crit}}^{(1)} = 0.2$  and  $\Theta_{\text{CO,crit}}^{(2)} = 0.5$ , are only determined with one significant figure and the quality of the fit can hardly be discussed. There is the possibility for an improvement in the values of the two critical coverages by generalizing the model and choosing instead of a single value ( $V$ ) different values for the transition rates for the two transitions  $\alpha\beta \rightarrow \beta\beta$  and  $\alpha\beta \rightarrow \alpha\alpha$ . This would lead to slightly different values for the critical coverages. To achieve this better fit one, however, requires the information on the critical coverages with an accuracy of at least two digits. This information is not available. This is why we have restricted our consideration to the basic questions concerning the mechanism of the reconstruction. But on the other hand our model gives the principal possibility to estimate the difference in the activation energies for the diffusion between the two surface phases. In experiment it should be very difficult or almost impossible to measure this value because this diffusion takes place only at the microscopic (i.e., atomic) length scale of the phase border. In the literature even the values determined for diffusion on a homogeneous surface phase vary by an order of magnitude [31] with the procedure of measurement. It would be interesting to compare our results with results of *ab initio* calculations for this process.

### C. Nucleation in the homogeneous phases

As shown above the heterogeneous state can be described without considering the nucleation process. The latter is only

necessary to create this heterogeneous state. But in the domain of the homogeneous phases for  $\Theta_A < \Theta_A^{(1)}(\kappa)$  or  $\Theta_A > \Theta_A^{(2)}(\kappa)$  the nucleation process is important to understand the critical surface activity and to explain the experimental results for the island growth rate obtained by Hopkinson *et al.* [14,15]. In the following, we restrict ourselves to the case  $\Theta_A < \Theta_A^{(1)}(\kappa)$ . In this case only the trivial solution  $\theta = \psi = 0$  exists for  $\gamma = 0$ . A weak nucleation  $\gamma \ll V$  creates a small induced solution  $\theta_{\text{ind}}$  and  $\psi_{\text{ind}}$ . In order to obtain a simple analytical solution we use the linearized equations, i.e., for  $\Theta_A = 0$  the homogeneous nucleation of  $\beta$  defects gives rise to an induced  $\beta$  phase coverage of

$$\Theta_{\beta}^{\text{ind}} = \theta_{\text{ind}} = \frac{\gamma}{V}.$$

The amplification in the creation of the  $\beta$  phase due to the presence of  $A$  can be expressed via the *effective nucleation rate*  $\gamma_{\text{eff}}$  given by

$$\gamma_{\text{eff}} = \Theta_{\beta}^{\text{ind}} V = \theta_{\text{ind}} V. \quad (11)$$

The amplification calculates to

$$\gamma_{\text{eff}}/\gamma = \frac{1}{\varepsilon} \left( \frac{1 + (1 - \varepsilon)\{2[1 - \Theta_A^{(1)}(\kappa)]^2 - 1\}}{1 - 2(1 - \varepsilon)[\Theta_A^{(1)}(\kappa)]^2} \right), \quad (12)$$

with

$$\varepsilon = 1 - \Theta_A/\Theta_A^{(1)}(\kappa). \quad (13)$$

This results in a singularity of the effective nucleation rate for  $\varepsilon \rightarrow 0$ . For  $\Theta_A = 0$  ( $\varepsilon = 1$ )  $\gamma_{\text{eff}}/\gamma = 1$  holds. In the approximation with the linearization with formally  $\gamma \rightarrow 0$  the local  $A$  coverage on the  $\alpha$  phase  $\Theta_A^{(\alpha)}$  is equal to the global  $A$  coverage  $\Theta_A$ . Because of finite values  $\gamma > 0$

$$\varepsilon = 1 - \Theta_A^{(\alpha)}/\Theta_A^{(1)}(\kappa) \quad (14)$$

should be used instead of Eq. (13) in the simulation.

Let us now shortly compare our model system with the model systems in the field of ferromagnetism, although the corresponding parameter actually is a vector. The critical point divides the paramagnetic domain (no magnetization,  $M = 0$ ) from the ferromagnetic domain (spontaneous magnetization,  $M \neq 0$ ). In our model there exist two critical values with a similar character. The first one  $\Theta_A^{(1)}(\kappa)$  divides the domain of the homogeneous  $\alpha$  phase ( $\Theta_{\beta} = 0$ ) from the heterogeneous stable state ( $\Theta_{\beta} \neq 0$ ). The second one  $\Theta_A^{(2)}(\kappa)$  separates the heterogeneous state and the homogeneous  $\beta$  phase ( $\Theta_{\alpha} = 0$ ). In the paramagnetic domain a weak external field creates the magnetization, and the ratio of these, the susceptibility, diverges at the critical point. In our model the nucleation as a weak internal process corresponds to the external field and the ratio  $\gamma_{\text{eff}}/\gamma$  in Eq. (12) corresponds to the susceptibility.

We therefore have a system with two critical points (for  $\kappa > 0$ ) each exhibiting a phase transition of second order, i.e., the phase coverages vary continuously at the critical points.

Furthermore, the effective nucleation rate [Eq. (12)] corresponds to a susceptibility that is typical for second-order phase transitions. For  $\kappa = 0$  the two critical points coincide. In the physically irrelevant interval  $-1 < \kappa < 0$  the phase transition is of first order. This can easily be seen from Eqs. (8) and (9) because now the upper critical value for the stability of the  $\alpha$  phase,  $\Theta_A^{(1)}(\kappa)$ , lies above the lower critical value for the stability of the  $\beta$  phase,  $\Theta_A^{(2)}(\kappa)$ . This then leads to hysteresis phenomena in MC simulations for  $\kappa < 0$ .

In the interval  $\Theta_A < \Theta_A^{(1)}(\kappa)$  some special properties exist. The nucleation in a homogeneous  $\alpha$  phase induces the  $\beta$  defects that are necessary for the growth of the  $\beta$  phase. The coverage of these defects is given by  $\Theta_A^{(\beta)} = \Theta_A \psi_{\text{ind}}/\theta_{\text{ind}}$  and therefore

$$\Theta_A^{(\beta)} = \Theta_A^{(2)}(\kappa) \frac{1 - \varepsilon}{1 - \varepsilon\{1 - 2[1 - \Theta_A^{(2)}(\kappa)]^2\}}. \quad (15)$$

The local coverage on the  $\beta$  phase increases monotonically and reaches its maximum  $\Theta_A^{(2)}(\kappa)$  at the critical point ( $\varepsilon = 0$ ). For larger coverages dynamically stable islands of both phases exist with constant local  $A$  coverages, i.e., the condition for the phase transition at  $\Theta_A = \Theta_A^{(1)}(\kappa)$  is that the local  $A$  coverage on the  $\beta$  defects in the  $\alpha$  phase created via homogeneous nucleation reaches a threshold coverage  $\Theta_A^{(\beta)} \geq \Theta_A^{(2)}(\kappa)$ , which is sufficient to induce the phase transition.

In the theory of phase transitions the MF approximation generally can only give the classic power law  $\varepsilon^{-x}$  with  $x = 1$  [see Eq. (12)]. Fluctuations, however, give rise to deviations of this power law. This can easily be shown via simulations of the present model system.

## V. SIMULATION

### A. Simulation without nucleation, $\gamma = 0$

In general, we use the artificial heterogeneous state with an equal amount of the  $\alpha$  and  $\beta$  phase distributed randomly over the lattice as the initial condition and therefore can neglect the nucleation process. Very surprisingly (at least for us), the simulation confirms the critical values, the validity of Eq. (10) as well as the values of the local coverages within an error of  $\mathcal{O}(V/D)$ . The agreement also holds for the simulation with a homogeneous  $\alpha$  or  $\beta$  phase as the initial condition with consideration of the nucleation (see below).

In Figs. 1 and 2 the homogeneous  $\alpha$  phase with a small  $\beta$  nucleus is chosen as the initial lattice condition for a clear presentation of the results. As can be clearly seen, the  $A$  particles are trapped on the initial nucleus of the  $\beta$  phase that in turn starts to grow to a certain size that depends on the total  $A$  coverage. The local  $A$  coverages on the individual phases are independent of the total  $A$  coverage. The  $\beta$  phase grows until saturation is obtained, i.e., until the ratio of the phase coverages corresponds to Eq. (10), because the probability to find  $A$  directly at the phase border does not lead to further growth of one or the other phase. It is important to note that the snapshots in Fig. 2 of the lattice are taken at short simulation times and do not show any segregation phe-

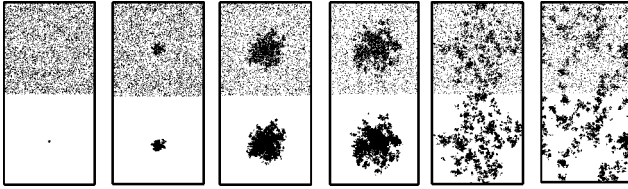


FIG. 1. Snapshots of the lattice during the growth of the  $\beta$  phase for  $\Theta_A=0.10$  and  $\kappa=0.9$ . The snapshots are taken at  $t=0, 100, 500, 1000, 10\,000,$  and  $25\,000$  (from left). The growth of the  $\beta$  phase (black in the lower part) because of trapping of  $A$  (black in the upper part) continues until the local coverages  $\Theta_A^{(\alpha)}$  and  $\Theta_A^{(\beta)}$  are equal to the critical coverages on the corresponding phases. For  $t>1000$ , the  $\beta$  coverage remains almost constant and the compact  $\beta$  phase dissolves into smaller islands that are homogeneous at the mesoscopic level.

nomena. For longer simulation times the compact structures of the individual surface phases will dissolve and cover the whole lattice (see Fig. 1). We here only show the compact structures at the beginning of the simulation for reasons of better comparison.

### B. Simulation with nucleation, $\gamma \neq 0$

Now we consider the homogeneous phase nucleation. This enables us to study the system in the whole parameter interval of the total  $A$  coverage  $\Theta_A$  because in the interval of the former homogeneous  $\alpha$  or  $\beta$  phase the nucleation creates small nuclei of the  $\beta$  or  $\alpha$  phase, respectively.

In Fig. 3 the phase diagram of our model system is shown. The coverage of the  $\beta$  phase  $\Theta_\beta$  and the local  $A$  coverages on the  $\alpha$  and  $\beta$  phase are shown as a function of the total  $A$  coverage  $\Theta_A$ . The lines give the results for different values of the parameter  $\kappa$  for the diffusion asymmetry with  $\kappa=0.0, 0.2, 0.4, 0.6,$  and  $0.8$  for lines 1–5, respectively. These are obtained from individual simulation runs for total  $A$  coverages in  $\Theta_A \in [0.005, 0.55]$  with step  $\Delta\Theta_A=0.005$ . Because the variations of the results are very small in the domain of the heterogeneous stable state, i.e., outside the domains I and II, we only show the lines without error bars. The simulations with nucleation somewhat extend the result given by Eq. (10) that only gives the phase coverages and the interval of the total  $A$  coverage  $\Theta_A$ , where the heteroge-

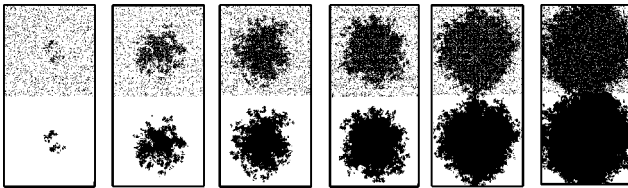


FIG. 2. Snapshots of the lattice for global  $A$  coverages (from left)  $\Theta_A=0.05, 0.10, 0.15, 0.20, 0.30,$  and  $0.40$  and  $\kappa=0.9$ . The snapshots are taken at  $t=1000$  and clearly show that only the coverage of the  $\beta$  phase (black in the lower part) depends on the global  $A$  coverage and that the local  $A$  (black in the upper part) coverages on the individual phases remain constant. The  $\beta$  islands dissolve at longer simulation times as shown in Fig. 1, but the coverage remains almost constant.

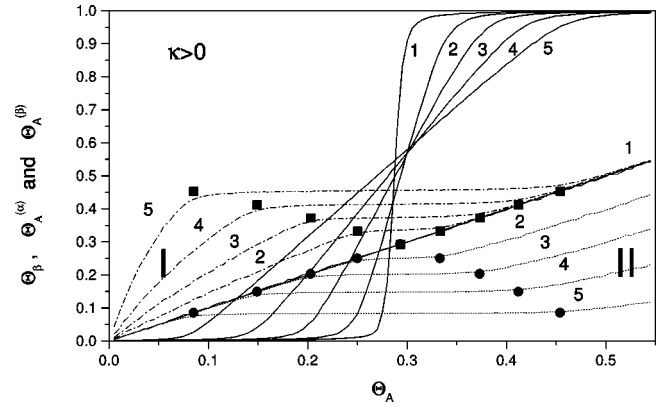


FIG. 3. The coverage of the  $\beta$  phase  $\Theta_\beta$  (solid) and the local  $A$  coverage on the  $\alpha$  (dotted) and  $\beta$  phase (dash-dotted) as a function of the total  $A$  coverage  $\Theta_A$ . The lines give the results for different values of the parameter  $\kappa$  for the diffusion asymmetry with  $\kappa=0.0, 0.2, 0.4, 0.6,$  and  $0.8$  for lines 1–5, respectively. The filled squares and circles give the stability border of the heterogeneous state without nucleation obtained by Eq. (10) [value on the  $x$  axis] and the local  $A$  coverages on the individual phases [value on the  $y$  axis].

neous state is stable even without nucleation. These results are shown by the squares and circles for the local  $A$  coverages on the  $\beta$  and  $\alpha$  phase, respectively. As can be seen, the error of the MF approximation is very small. Even in domains I and II the error of Eq. (15) is only about 10%. One very interesting aspect is that the lines of the  $\beta$  phase coverage cross each other at  $\Theta_A \approx 0.3$  with  $\Theta_\alpha \approx \Theta_\beta \approx 0.5$ . This is in excellent agreement with the experimental value of  $\Theta_{CO} \approx 0.3$  determined by Thiel *et al.* [3] for which the reconstructed and nonreconstructed phases are energetically equivalent and both phases have similar coverages. The domains I and II correspond to the domain of the homogeneous  $\alpha$  and  $\beta$  phase, respectively, if nucleation would not be considered. In these domains the density of the small defect islands due to nucleation is small and statistical fluctuations are rather large. The size of these fluctuations can be seen in Fig. 4, where the effective nucleation rate is shown as a function of the local  $A$  coverage on the  $\alpha$  phase for different values of  $\kappa$ . In this case the error of the MF approximation is quite large. This can be seen for  $\kappa=0$  where MF predicts much lower values than the correct simulation results.

The results for different values of  $\kappa$  can be fitted with  $\gamma/\gamma_{\text{eff}}=c\varepsilon^\delta$ . The mean value of the constant parameter  $c$  is  $c=0.97 \pm 0.02$ . Therefore we can use  $c=1$  as an approximation. The exponent  $\delta$  shows a distinct dependence on the parameter  $\kappa$  and can be given by

$$\delta = \delta(\kappa) \approx a_0 + a_1 \kappa,$$

with  $a_0 = 1.29 \pm 0.02$  and  $a_1 = 0.39 \pm 0.04$ . The simulation results for different values of  $\kappa$  are summarized in Fig. 5. This renders possible a quantitative comparison with the experimental results [14,15] for the island growth rate of the  $1 \times 1$  ( $\beta$ ) phase on Pt(100).

(i) In Fig. 2 of Ref. [14] the island growth rate is shown as a function of the local CO coverage on the *hex* phase. In this

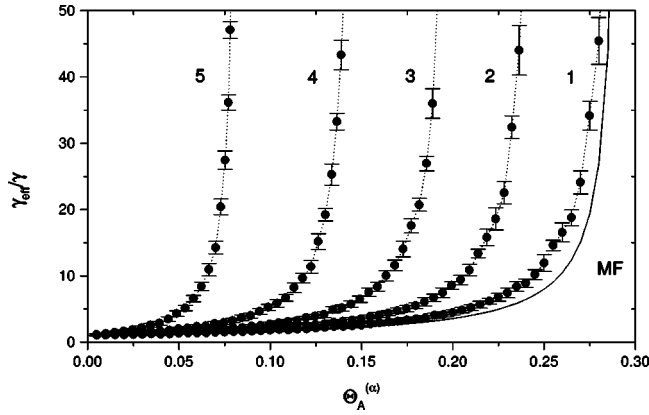


FIG. 4. Effective nucleation rate  $\gamma_{\text{eff}}/\gamma$  as a function of the local  $A$  coverage on the  $\alpha$  phase for different values of the parameter  $\kappa$  for the diffusion asymmetry with  $\kappa=0.0, 0.2, 0.4, 0.6,$  and  $0.8$  for lines 1–5, respectively. The error bars give the mean square deviation. The solid line on the right give the result of the MF approximation for  $\kappa=0$ .

figure the island growth rate has been measured up to a maximum local CO coverage of  $\Theta_{\text{CO,max}}^{(\text{hex})} = 0.03$  and increases nonlinearly in very good agreement with Fig. 4 in our present paper. Comparing these two figures we assume that the critical CO coverage in the experiments by Hopkinson *et al.* [14,15], which have been performed at temperatures around 400 K should be slightly larger than the maximum of the local CO coverage determined in the experiment  $\Theta_{\text{CO,crit}}^{(\text{hex})} > \Theta_{\text{CO,max}}^{(\text{hex})} = 0.03$ .

(ii) In the interpretation of the experimental results the growth rate has been fitted as a very nonlinear function of the local  $A$  coverage on the  $\text{hex}$  phase. The nonlinear fit gives an exponential dependence as a result and it was stated that the growth rate  $r_g$  apparently obeys a power law  $r_g \propto [\Theta_{\text{CO}}^{(\text{hex})}]^\nu$  with an exponent of  $\nu=4.5 \pm 0.4$  with respect to the CO coverage on the  $\text{hex}$  phase [15]. This is possible and has been used in subsequent papers [32–35] as a parameter in the so-called mathematical modeling based on the MF approximation. As has been shown in our previous study [28]

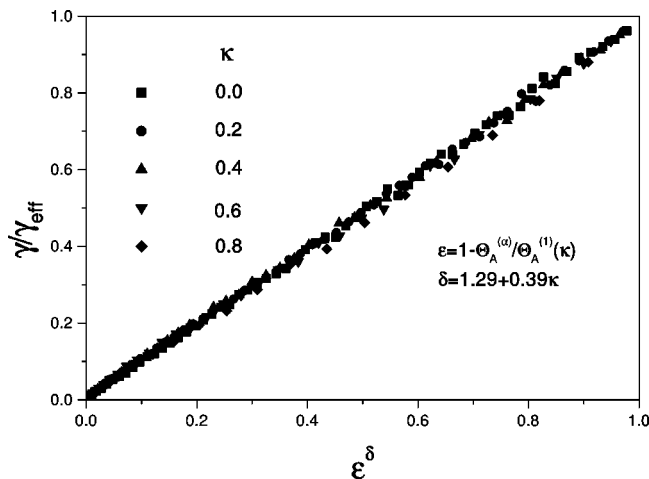


FIG. 5. The ratio  $\gamma/\gamma_{\text{eff}}$  (reciprocal of the effective nucleation rate) as a function of  $\epsilon^\delta$ .

our model can give exponents of  $\nu \approx 4-10$  [see point (b) below]. But some remarks have to be mentioned.

(a) This nonlinear fit to  $r_g \propto [\Theta_{\text{CO}}^{(\text{hex})}]^\nu$  in Refs. [14,15] or to  $\gamma_{\text{eff}}/\gamma \propto [\Theta_A^{(\alpha)}]^\nu$  in the present study is certainly feasible but as has been shown above the study of the dependence on  $\epsilon$  is the more correct approach than of the dependence on the local CO ( $A$ ) coverage.

(b) In the nonlinear fit procedure the largest values of the growth rate ( $r_g$  or  $\gamma_{\text{eff}}/\gamma$ ) dominate the value of the exponent  $\nu$ . This is the basic reason for the apparent temperature dependence of the growth rate in Refs. [14,15] where the exponent  $\nu$  has been determined to 3.9, 4.7, 5.4, and 5.8 at 380 K, 390 K, 400 K, and 410 K, respectively, because for the higher temperature values larger local CO coverages and larger island growth rates have been used in the fit procedure. These exponents are combined to  $\nu=4.5 \pm 0.4$  because the temperature dependence was deemed not to be significant within experimental error.

(c) The fit to a nonlinear function in the local CO coverage as well as the mathematical modeling for the macroscopic kinetics using this nonlinear function can be performed. But the *microscopic* interpretation that 4–5 CO molecules are necessary in a concerted reaction step to induce the  $\text{hex} \rightarrow 1 \times 1$  transition and therefore the conclusion that the *microscopic* island growth is also a strongly nonlinear phenomenon is not acceptable.

## VI. CONCLUSIONS

Our model is able to explain the most important phenomena such as the island growth rate and the existence of critical adsorbate coverages that have been observed in experiments investigating the reconstruction of the Pt(100) and Pt(110) single crystal surfaces. The basic mechanism is identical on both surfaces, but a relatively small quantitative difference in the activation energy of the adsorbate surface diffusion for jumps from one surface phase to the other leads to a very different behavior.

Homogeneous surface phase nucleation creates small phase defects due to thermal fluctuations in otherwise homogeneous surface phases of the reconstructed ( $\alpha$ ) or nonreconstructed ( $\beta$ ) surface, respectively. These defects can grow or decline in dependence of the very local adsorbate coverage, i.e., only the presence or absence of adsorbate particles directly at the phase border determines the evolution of the individual surface phase islands. In this context, it is important to note that both processes the nucleation and the phase border propagation show *linear* kinetics on the microscopic (atomic) length scale, which give rise to nonlinear phenomena in the macroscopic island growth rate. The homogeneous nucleation in combination with the island growth via phase border propagation is the basic underlying mechanism of surface reconstruction. The difference in the adsorption energy on the  $\alpha$  and  $\beta$  surface phase leads to an asymmetry in the adsorbate diffusion. The adsorbate particles are trapped on the  $\beta$  phase, i.e., jumps from the  $\beta$  to the  $\alpha$  phase are hindered compared to jumps in the reverse direction. This leads to two critical adsorbate coverages  $\Theta_A^{(1)}$  and  $\Theta_A^{(2)}$  that

determine the stability of the individual phases. For  $\Theta_A < \Theta_A^{(1)}$  the  $\alpha$  phase and for  $\Theta_A > \Theta_A^{(2)}$  the  $\beta$  is stable. A dynamically stable heterogeneous state exists for  $\Theta_A^{(1)} < \Theta_A < \Theta_A^{(2)}$ . In this interval the local adsorbate coverages are independent of the total adsorbate coverage and only the amount of the individual phases varies. Both phase transitions occurring at these critical values are of second order. The diffusion asymmetry can be expressed via an additional parameter  $\kappa$ . It is only the value of  $\kappa$  that determines the critical values  $\Theta_A^{(1)}$  and  $\Theta_A^{(2)}$ , i.e., the difference in the value

of  $\kappa$  is the reason for different quantitative behavior of the surface reconstruction on Pt(100) and Pt(110).

#### ACKNOWLEDGMENTS

The authors acknowledge financial support from the Deutsche Forschungsgemeinschaft for O.K. and V.K. Part of this work was supported by the Fonds der Chemischen Industrie and the European Center of Excellence in Advanced Materials Research and Technology (Contract No. ICA-1-CT-2000-7007).

- 
- [1] C. M. Comrie and L. M. Lambert, *J. Chem., Soc., Faraday Trans. 1* **72**, 1659 (1976).
- [2] R. J. Behm, P. A. Thiel, P. R. Norton, and G. Ertl, *J. Chem. Phys.* **78**, 7437 (1983).
- [3] P. A. Thiel, R. J. Behm, P. R. Norton, and G. Ertl, *J. Chem. Phys.* **78**, 7448 (1983).
- [4] T. Gritsch, D. Coulman, R. J. Behm, and G. Ertl, *Phys. Rev. Lett.* **63**, 1086 (1989).
- [5] *The Chemical Physics of Solid Surfaces*, edited by D. A. King and D. P. Woodruff (Elsevier, Amsterdam, 1994), Vol. 7.
- [6] R. Imbihl and G. Ertl, *Chem. Rev.* **95**, 697 (1995).
- [7] V. P. Zhdanov and B. Kasemo, *J. Stat. Phys.* **90**, 79 (1998).
- [8] V. P. Zhdanov, *J. Chem. Phys.* **110**, 8748 (1999).
- [9] R. Imbihl, M. P. Cox, G. Ertl, H. Müller, and W. Brenig, *J. Chem. Phys.* **83**, 1578 (1985).
- [10] K. Krischer, M. Eiswirth, and G. Ertl, *J. Chem. Phys.* **97**, 307 (1992).
- [11] R. Imbihl, S. Ladas, and G. Ertl, *Surf. Sci.* **206**, L903 (1988).
- [12] M. Kim, W. S. Sim, and D. A. King, *J. Chem. Soc., Faraday Trans.* **92**, 4781 (1996).
- [13] T. E. Jackman, K. Griffith, J. A. Davies, and P. R. Norton, *J. Chem. Phys.* **79**, 3529 (1983).
- [14] A. Hopkinson, J. M. Bradley, X.-C. Guo, and D. A. King, *Phys. Rev. Lett.* **71**, 1597 (1993).
- [15] A. Hopkinson, X.-C. Guo, J. M. Bradley, and D. A. King, *J. Chem. Phys.* **99**, 8262 (1993).
- [16] E. Ritter, R. J. Behm, G. Pötschke, and J. Winterlin, *Surf. Sci.* **181**, 403 (1987).
- [17] V. P. Zhdanov, *Surf. Sci.* **426**, 345 (1999).
- [18] V. N. Kuzovkov, O. Kortlüke, and W. von Niessen, *J. Chem. Phys.* **108**, 5571 (1998).
- [19] O. Kortlüke, V. N. Kuzovkov, and W. von Niessen, *J. Chem. Phys.* **110**, 11523 (1999).
- [20] O. Kortlüke, V. N. Kuzovkov, and W. von Niessen, *Phys. Rev. Lett.* **83**, 3089 (1999).
- [21] O. Kortlüke, V. N. Kuzovkov, and W. von Niessen, *Phys. Rev. Lett.* **81**, 2164 (1998).
- [22] R. J. Gelten, A. P. J. Jansen, R. A. van Santen, J. J. Lukien, J. P. L. Segers, and P. A. J. Hilbers, *J. Chem. Phys.* **108**, 5921 (1998).
- [23] E. V. Albano, *Langmuir* **13**, 4013 (1997).
- [24] E. V. Albano, *J. Chem. Phys.* **109**, 7498 (1998).
- [25] G. Zvejnicks and V. N. Kuzovkov, *Phys. Rev. E* **63**, 051104 (2001).
- [26] R. M. Ziff, E. Gulari, and Z. Barshad, *Phys. Rev. Lett.* **56**, 2553 (1986).
- [27] P. Meakin and D. Scalapino, *J. Chem. Phys.* **87**, 731 (1987).
- [28] V. N. Kuzovkov, O. Kortlüke, and W. von Niessen, *Phys. Rev. Lett.* **83**, 1636 (1999).
- [29] V. N. Kuzovkov, O. Kortlüke, and W. von Niessen, *Phys. Rev. E* **63**, 023101 (2001).
- [30] O. Kortlüke, *J. Phys. A* **31**, 9185 (1998).
- [31] V. J. Kwasniewski and L. D. Schmidt, *Surf. Sci.* **274**, 329 (1992).
- [32] A. Hopkinson and D. A. King, *Chem. Phys.* **177**, 433 (1993).
- [33] D. A. King, *Surf. Rev. Lett.* **1**, 435 (1994).
- [34] M. Gruyters, T. Ali, and D. A. King, *Chem. Phys. Lett.* **232**, 1 (1995).
- [35] M. Gruyters, T. Ali, and D. A. King, *J. Phys. Chem.* **100**, 14417 (1996).